Analytical Model of the Three-Dimensional Plasmonic Ruler

Timothy J. Davis,[†,*] Mario Hentschel,[‡,∥] Na Liu,[§] and Harald Giessen[‡]

[†]CSIRO, Materials Science and Engineering, Private Bag 33, Clayton, VIC, 3168, Australia, [‡]4th Physics Institute and Research Center SCoPE, University of Stuttgart, Pfaffenwaldring 57, 70563 Stuttgart, Germany, [§]Department of Electrical and Computer Engineering, Rice University, 600 Main Street, Houston, Texas 77005, United States, and [∥]Max Planck Institute for Solid State Research, Heisenbergstraße 1, 70563 Stuttgart, Germany

ABSTRACT

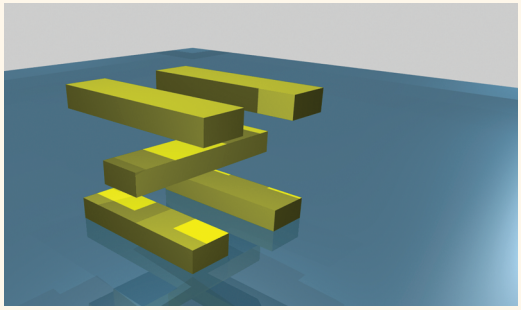

An electrostatic eigenmode method that describes the coupling between plasmonic nanoparticles is used to model the optical resonances of the 3D plasmonic ruler. The model provides a mathematical description of the ruler that enables us to identify the key resonance in the scattering spectrum that encodes the location of the central nanorod. The model demonstrates excellent agreement with experimentally measured spectra. We show that the spectra can uniquely encode the horizontal and vertical displacements of the central nanorod. From an understanding of the spatial dependence of the plasmonic coupling between the nanorods, we devise a method for estimating the position of the central nanorod and apply this to experimental data. Our method paves the way toward the use of high-resolution spectra from 3D plasmonic oligomers for structural analysis of single entities such as complex macromolecules, DNA scaffolds, proteins, and peptides.

KEYWORDS: plasmon ruler · nanoparticle coupling · localized surface plasmons · induced transparency · optical antenna

Localized surface plasmons are charge oscillations that can be excited optically on the surfaces of metallic nanoparticles. When the nanoparticles are in close proximity, there is an interaction between the localized surface plasmons that is mediated by their electric fields, resulting in a Coulomb-like coupling between them. The spatial variation of the electric field gives rise to a spatial dependence of the interaction, leading to optical resonances that depend on the distance between the nanoparticles. This effect has been used to create a plasmonic ruler.[1−4] When the metal nanoparticles are combined with molecular systems, the plasmonic interaction and the subsequent change in the optical spectrum yields information about the separation of the molecules or the components of large polymer chains. Recently, this idea was extended to three dimensions[5] using a more complex nanoparticle structure that is sensitive to both separation and translation. This three-dimensional plasmonic ruler exploits the presence of two subradiative plasmonic resonances excited by near-field coupling to a plasmonic dipole antenna. The nonradiative resonances are formed by the interaction between pairs of metal nanorods that lead to a quadrupole resonance with low scattering.[6] Energy from the dipole antenna couples into the quadrupole mode, which results in a drop in the overall scattered intensity and an increase in the transmittance, an effect which is known as plasmon-induced transparency.[7−13] When two such subradiative structures are formed, it has been shown that the location of the centrally placed excitation dipole controls the intensity and frequency of features in the scattering spectrum. In this way, the plasmonic structure behaves like a ruler providing a measure of the displacement of the central antenna. The potential applications of this structure are in biology and complex macromolecular processes where the conformation of the molecules and their variation with time are important.

There are several important issues relating to the use of the three-dimensional plasmonic ruler. The first issue concerns the ability of the ruler to uniquely encode both the horizontal (*S*) and vertical (*H*) displacements of the central nanorod. That is, for these two parameters to be extracted from the optical spectrum, they must affect the spectral features in different and separable ways. Second, for the three-dimensional plasmonic ruler to be useful, we require some method of calibration, so

* Address correspondence to tj.davis@csiro.au.

Received for review October 19, 2011 and accepted January 6, 2012.

Published online January 06, 2012
10.1021/nn204029p

that the displacements are known either in absolute units (such as nanometers) or as relative displacements. In this paper, we use a mathematical approach to analyze the scattering spectra from the three-dimensional plasmonic ruler and show that both issues, that of uniqueness and calibration, can be satisfied. We use an electrostatic method to model the coupling of the localized surface plasmons in the nanorods and derive the relationships between the Coulomb coupling coefficients and the resonant frequencies of the modes in the structure. This allows us to identify the resonance of the central nanorod as the key feature in the optical spectrum that encodes the horizontal and vertical displacement which separately affect the frequency of the resonance and its strength. We show that it is possible to design the ruler so that linear combinations of the coupling coefficients depend only on one or the other of the displacements, thereby allowing these parameters to be calculated from measurements of the optical spectrum. Moreover, we derive an approximate relationship linking the coupling coefficients to the displacements of the central nanorod, and we use this relation to estimate the vertical and horizontal position of the nanorod from the measured transmission spectra. The change in the position of the central nanorod is known in absolute units if its initial position is known, which provides one method for calibrating the ruler.

RESULTS AND DISCUSSION

The configuration of the plasmonic ruler that we consider is shown in Figure 1. It consists of two pairs of parallel nanorods that are each associated with a nonradiative quadrupole moment. The fifth nanorod acts like an antenna in which a dipole mode is excited by the incident light polarized parallel to its long axis. This central dipole antenna scatters the incident light but is also coupled to the two quadrupole structures that absorb energy from it. The interaction leads to the change in the scattering spectrum and is responsible for the induced transparency. Displacements *S* and *H* of the antenna alter the relative strengths of the coupling, causing changes in the scattering spectrum. The first question we wish to answer is: *can the spectrum uniquely encode S and H separately?* For our analysis, we make a number of simplifying assumptions. For the situation where the structure is very much smaller than the wavelength of light, we assume that retardation is not dominant and use an electrostatic method which allows us to develop a mathematical model of the ruler.[14,15] This method has been shown previously to reproduce the features of induced transparency and Fano resonances.[15]

In the electrostatic eigenmode model, the interaction between nanoparticles is described in terms of the Coulomb forces associated with the surface charges. These electric charges represent the localized surface plasmon (LSP) modes in the nanoparticles. The spatial

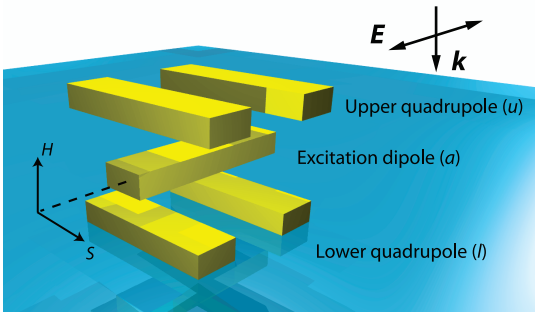

Figure 1. Three-dimensional plasmonic ruler consists of two pairs of metal nanorods (upper and lower) and a central dipole antenna. The antenna excites subradiative quadrupole modes in the two pairs of nanorods. The scattering spectrum changes with the lateral *S* and vertical *H* displacements of the antenna. The optical excitation has the electric field aligned with the central nanorod and it is incident from above.

dependence of the Coulomb coupling between the different elements of the ruler is described by a geometric coupling coefficient *G* that represents the interaction between pairs of nanorods. It depends on the nanorod separation. It has been shown[15] that, to lowest order, the geometric coupling G_{rq} between nanoparticles *r* and *q* has the form of an electric dipole−dipole coupling

$$G_{rq} \propto d_{rq}^{-3}(3(\vec{p}_r \cdot \hat{d})(\vec{p}_q \cdot \hat{d}) - (\vec{p}_r \cdot \vec{p}_q)) \qquad (1)$$

where $\vec{p}_r$ is the dipole moment of the resonant mode of particle *r*, d_{rq} is the distance between the two particles, and $\hat{d}$ is a unit vector pointing from particle *r* to *q*. From this equation, we see that the geometric coupling is symmetric, $G_{rq} = G_{qr}$, and has a sign that depends on the relative orientation of the dipole moments and the displacement of the nanoparticles. It is this geometric dependence of the coupling that is exploited in the plasmon ruler. A schematic representation of the coupling is shown in Figure 2 where eq 1 is used to determine the signs of the coefficients. Here we assume that the direct coupling between the upper quadrupole and the lower quadrupole is negligible. Since these structures are fixed with respect to one another, any coupling between them will mainly induce a fixed shift in their resonances which does not affect the operation of the ruler. This point is explained more extensively below. Note that it is possible that many resonant modes are being excited in each nanoparticle. However, for simplicity, we have assumed that only one of these modes is dominant.

A light field of frequency ω applied to an isolated nanoparticle *r* will excite a localized surface plasmon resonance with an amplitude $a_r(\omega)$. However, the Coulomb coupling from nearby nanoparticles changes the excitation amplitude, now represented by $\tilde{a}_r(\omega)$. The electrostatic coupling model provides a simple way of representing the excitations in a coupled system of plasmonic nanoparticles in terms of the optical excitation of each nanoparticle when isolated. The interactions are obtained from a matrix equation linking

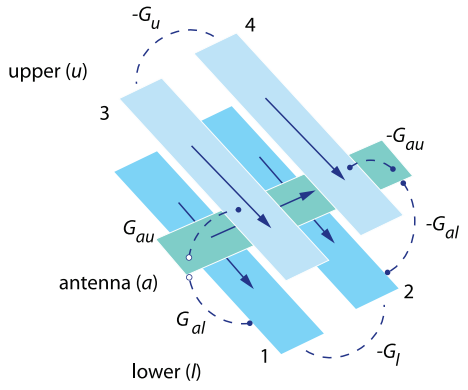

Figure 2. Schematic diagram of the coupling between the different nanorods. The arrows reference the positive direction of the dipole moments in each nanorod. The signs of the geometric coupling coefficients G vary depending on whether the dipole moments couple head-to-tail or head-to-head/tail-to-tail.

the coupled amplitudes $\tilde{a}_r$ to the uncoupled amplitudes a_r. The matrix depends on the coupling coefficients C_{rq} that include the geometric coupling G_{rq} and a term that depends on the resonant frequency ω_r of the LSP mode of particle r. If we include a complex Drude damping term $i\Gamma/2$, then we can write the coupling coefficients in the form $C_{rq} = -G_{rq}/(\omega - \omega_r + i\Gamma/2)$. With this in mind, we have the following relations: $C_{a1} = -C_{a2}$, $C_{a3} = -C_{a4}$, $C_{1a} = -C_{2a}$, $C_{3a} = -C_{4a}$, $C_{12} = C_{21}$, and $C_{34} = C_{43}$. The matrix equation describing the coupling in the ruler then has the form

$$\begin{pmatrix} \tilde{a}_a \\ \tilde{a}_1 \\ \tilde{a}_2 \\ \tilde{a}_3 \\ \tilde{a}_4 \end{pmatrix} = \begin{pmatrix} 1 & -C_{a1} & C_{a1} & -C_{a3} & C_{a3} \\ -C_{1a} & 1 & -C_{12} & 0 & 0 \\ C_{1a} & -C_{12} & 1 & 0 & 0 \\ -C_{3a} & 0 & 0 & 1 & -C_{34} \\ C_{3a} & 0 & 0 & -C_{34} & 1 \end{pmatrix}^{-1} \begin{pmatrix} a_a \\ a_1 \\ a_2 \\ a_3 \\ a_4 \end{pmatrix} \quad (2)$$

To solve this equation, we invert the matrix and multiply the result into the column vector on the right. This vector contains the amplitudes of the nanoparticles when they are not coupled. Since the applied electric field is polarized parallel to the center dipole antenna, none of the other nanoparticles will be excited directly, so that $a_1 = a_2 = a_3 = a_4 = 0$. The excitation of the antenna a_a when isolated is given by $a_a = -A_a/(\omega - \omega_a + i\Gamma/2)$, which depends on its resonance frequency ω_a and a constant A_a. Solving eq 2 yields the excitation amplitude of the antenna when coupled to the other nanorods. This has the form $\tilde{a}_a = A_a/\Delta$, where

$$\Delta = \frac{2G_{al}^2}{(\omega - \omega_{ql} + i\Gamma/2)} + \frac{2G_{au}^2}{(\omega - \omega_{qu} + i\Gamma/2)} - (\omega - \omega_a + i\Gamma/2) \quad (3)$$

Here, $\omega_{ql} = \omega_l + G_l$ and $\omega_{qu} = \omega_u + G_u$ are the resonance frequencies of the quadrupoles formed by the lower and upper pairs of nanorods, respectively. We have assumed that the rods all have the same damping factor Γ. The scattering spectrum is proportional to $|\tilde{a}_a|^2 = A_a^2/|\Delta|^2$, and the transmission spectrum is approximately $I_{max} - A_a^2/|\Delta|^2$. We have fitted this expression for the transmission to the published data of Liu *et al.*[5] These data consist of experimentally measured spectra from a set of rulers with different lateral displacements S of the central nanorod. However, in the absence of experimental spectra for vertical displacements H, we also fit our model to the numerical simulations of Liu *et al.*[5] These spectra are shown in Figure 3 along with the fits of our analytical model. (The important fitted parameters are given in Table 1 and Table 2.) The analytical model fits very well the experimental spectra for different offsets S of the antenna. However, for the numerical data, the fits are best for the antenna displaced between $H = -10$ nm and $H = 5$ nm and show reduced accuracy for larger displacements. This may be due to the interaction between higher-order resonant modes that are taken into account in the numerical model but have been neglected in our analysis. Evidence for this is seen in the relatively straight slope of the transmission spectrum between the two main resonances when the displacement of the antenna is large. This is particularly obvious for $H = 15$ nm where the central resonance is a relatively small feature. In contrast, our analytical model produces large smooth curves that are not able to reproduce this feature. This impacts our ability to recover the position of the antenna over a large vertical displacement, as discussed below.

Since the scattering spectrum is proportional to $|\tilde{a}_a|^2 = A_a^2/|\Delta|^2$, the scattering is a minimum (transmission is a maximum) when either $\omega = \omega_{ql}$ or $\omega = \omega_{qu}$, which corresponds to the resonances of the lower and upper quadrupoles. This can be seen from eq 3 by ignoring the losses, $\Gamma = 0$, for then Δ is infinite at the resonances and therefore $\tilde{a}_a = A_a/\Delta = 0$. These minima, which are associated with the plasmon-induced transparent maxima, depend on the coupling within the nanoparticle pairs, through coefficients G_l and G_u, but do not depend on the position of the dipole antenna except for a partial overlap of the resonances due to their finite width. In this regard, these minima are not ideal reference points for monitoring the position of the center dipole, as was suggested by Liu *et al.*[5]

On the contrary, the frequencies of the scattering resonances or transmission minima, and particularly the center resonance, depend on the coupling between the antenna and the quadrupoles. It is the position dependence of this coupling that encodes the location of the antenna in the scattering spectrum. These resonances occur when $|\Delta|^2$ is small. If we treat the resonance frequencies as complex numbers, such that $\tilde{\omega}_{ql} = \omega_{ql} - i\Gamma/2$ and similarly for $\tilde{\omega}_{qu}$ and $\tilde{\omega}_a$, then the resonances occur when $\Delta = 0$. This leads to a cubic equation with three solutions corresponding to

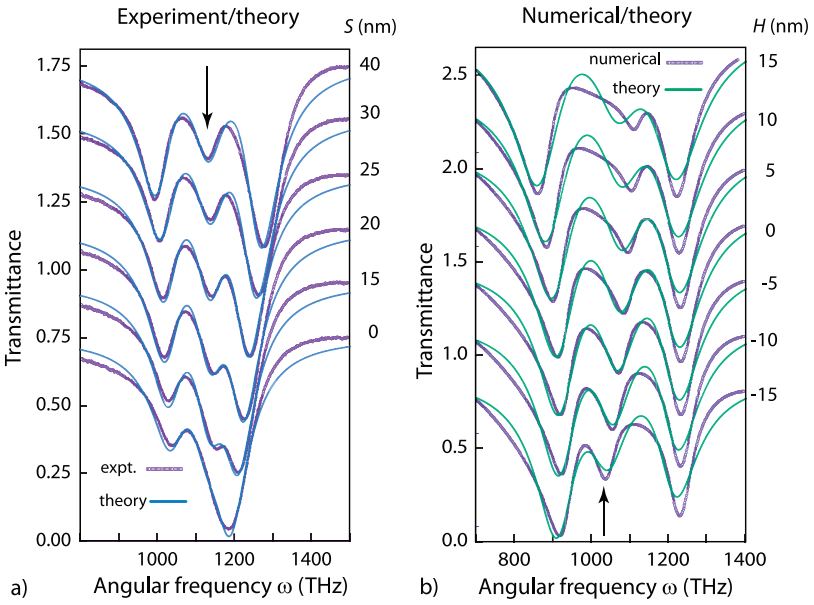

Figure 3. Comparisons between the spectra associated with the plasmonic ruler and the analytical expression for the scattering for different positions of the central dipole antenna: (a) experimental data from Liu *et al.*[5] and our analytical model fitted to the data for different lateral translations *S* of the antenna; (b) numerical data and fits of our analytical model for different vertical displacements *H* of the antenna. In all cases, the transmittance data have been fitted to $I_{max} - A_a^2/|\Delta|^2$, where I_{max} as well as A_a, G_{al}, G_{au}, ω_{ql}, ω_{qu}, ω_a, and Γ were adjustable parameters. The arrows show the frequency of the central resonance that encodes the location of the dipole antenna. The transmittance spectra have been offset for clarity.

TABLE 1. Fit Parameters for Figure 3a,[a]

S (nm)	G_{al}	G_{au}	ω_{ql}	ω_a	ω_{qu}	Γ
0	22.8	36.8	1151	1129	1076	105
15	27.7	39.1	1171	1133	1074	99
20	33.1	44.3	1178	1135	1073	99
25	38.6	45.8	1183	1140	1071	96
30	46.4	50.9	1191	1148	1069	101
40	53.7	55.5	1194	1146	1063	102

[a] Except for the displacement *S*, all parameters are in THz. The upper nanorod pair is offset in *S* by 35 nm, and the central rod is placed midway between both nanorod pairs, at a vertical distance of 70 nm measured between the centers of the nanorods.

TABLE 2. Fit Parameters for Figure 3b,[a]

H (nm)	G_{al}	G_{au}	ω_{ql}	ω_a	ω_{qu}	Γ
−20	74.1	56.4	1122	1029	979	133
−15	69.9	53.3	1134	1049	983	123
−10	65.7	55.8	1143	1060	988	120
−5	62.5	60.2	1148	1064	991	121
0	60.5	65.3	1151	1065	992	126
5	59.8	71.0	1151	1061	989	132
10	60.2	76.8	1146	1052	982	141
15	62.3	82.1	1136	1038	969	150
20	67.1	88.0	1119	1016	946	158

[a] Except for the displacement *H*, all parameters are in THz. The central rod is offset vertically by 70 nm, as measured from the centers of the nanorods, and horizontally by 85 nm from the center of the upper nanorod pair and 50 nm from the lower pair.

the three main scattering resonances in this system. The solution of the cubic equation is rather complicated, but we can derive an approximate solution for the center resonance. Since this resonance is close to that of the antenna resonance, we consider the deviation $\delta\omega = \omega - \tilde{\omega}_a$. The first order expression for $\delta\omega$ depends on frequency differences, such as $\tilde{\omega}_{qu} - \tilde{\omega}_a = \omega_{qu} - \omega_a$, which are real quantities, because the imaginary terms cancel. Therefore, we find that the frequency of the center resonance ω_R depends on the coupling coefficients approximately as

$$\omega_R \approx \omega_a + \frac{2G_{au}^2(\omega_{ql} - \omega_a) - 2G_{al}^2(\omega_a - \omega_{qu})}{(\omega_{ql} - \omega_a)(\omega_a - \omega_{qu}) + 2(G_{al}^2 + G_{au}^2)} \quad (4)$$

Here we assume that the lower quadrupole resonance is at a higher frequency than the center dipole, so that $\omega_{ql} - \omega_a > 0$, and that the upper quadrupole has a lower frequency, so that $\omega_a - \omega_{qu} > 0$. The minus sign between the two terms in the numerator of eq 4 then controls how the resonance frequency varies with the coupling to the upper and lower quadrupoles. This allows us to define a *balanced condition* when $G_{au}^2(\omega_{ql} - \omega_a) = G_{al}^2(\omega_a - \omega_{qu})$ so that the effects of the coupling to the quadrupoles cancel and the resonance of the dipole antenna remains at $\omega_R = \omega_a$. If the coupling coefficients change by a similar amount under some perturbation, such as a horizontal translation *S* of the dipole antenna, then the center resonance does not change and the spectrum is insensitive to this motion. Alternatively, if the coupling coefficients change in an opposite way, such as with a vertical displacement *H* of the antenna, then the center resonance

changes and provides a measure of this motion. When compared with the actual frequency of the center resonance for a range of coupling coefficients, the errors arising from eq 4 are found to be less than about 0.5%.

From the previous discussion, we know that when the loss Γ is small then the resonance corresponds to $Re\Delta(\omega_R) \approx 0$ so that $\Delta(\omega_R) \approx \mathrm{Im}\Delta(\omega_R)$. If we measure the intensity of the scattering at the resonance ω_R, then the amplitude depends only on $|\tilde{a}_a(\omega_R)|^2 \approx A_a^2/(\mathrm{Im}\Delta(\omega_R))^2$, where $\mathrm{Im}\Delta(\omega_R)$ is given by

$$\mathrm{Im}\,\Delta(w_R) = -(\Gamma/2)\left(\frac{2G_{al}^2}{(\omega_R-\omega_{ql})^2+\Gamma^2/4}+\frac{2G_{au}^2}{(\omega_R-\omega_{qu})^2+\Gamma^2/4}+1\right) \quad (5)$$

Changes to the intensity are found by taking the derivative with respect to some parameter P, which could represent the lateral displacement S of the antenna, with the result

$$\frac{d|\tilde{a}_a(\omega_R)|^2}{dP} \approx \frac{2\Gamma|\tilde{a}_a(\omega_R)|^2}{\mathrm{Im}\,\Delta(\omega_R)} \times\left(\frac{G_{al}}{(\omega_R-\omega_{ql})^2+\Gamma^2/4}\frac{dG_{al}}{dP}+\frac{G_{au}}{(\omega_R-\omega_{qu})^2+\Gamma^2/4}\frac{dG_{au}}{dP}\right) \quad (6)$$

Unlike the resonance frequency, the scattering at resonance $|\tilde{a}_a(\omega_R)|^2$ is controlled by a positive sign between the two coupling terms. It has a larger change if the two coupling coefficients vary the same way with parameter P.

The scattering intensity at resonance and the resonance frequency have been evaluated for a range of coupling coefficients similar to those obtained from the fits in Figure 3, with the results shown in Figure 4. This clearly shows that the intensity and resonance frequency of the center scattering peak depend on the coupling coefficients in an approximately orthogonal manner. For example, referring to Figure 4a, if G_{au} changes with G_{al} so that a particular contour is followed, then the intensity of the scattering peak of the central resonance does not change, whereas the resonance frequency does change, leading to frequency shifts similar to those shown in Figure 3a. More generally, provided that the coupling coefficients depend on the position of the center dipole antenna in such a way that nonparallel contours are followed, then it should be possible to obtain both the translation S and the vertical displacement H independently.

These results, in part, answer the question we posed earlier in that the variations of the coupling coefficients are uniquely encoded in the scattering spectra. It remains to be demonstrated how the coupling coefficients vary with the position S and H of the antenna. This is also related to the practical situation of determining the displacement of the central nanorod from a measurement of the scattering spectrum. This can be done in several ways. First, eq 3 can be fitted to the spectrum and the coupling coefficients G determined. If we know how these coefficients depend on distance, then the position of the central nanorod can be determined. Second, we can use the approximate forms eq 4 and eq 6 to relate the frequency and amplitude shifts of the central resonance to the changes in the coupling coefficients, but, again, we require some knowledge of how these coefficients depend on position.

A mathematical expression for the dependence of the coupling on the position of the central nanorod is difficult to obtain. In the electrostatic formalism, the coupling depends on the eigenfunctions associated with the resonant modes. In this formalism, the interaction between the nanorods is purely Coulombic and it is given in terms of the electric field from a surface charge distribution σ_a on particle a interacting with the

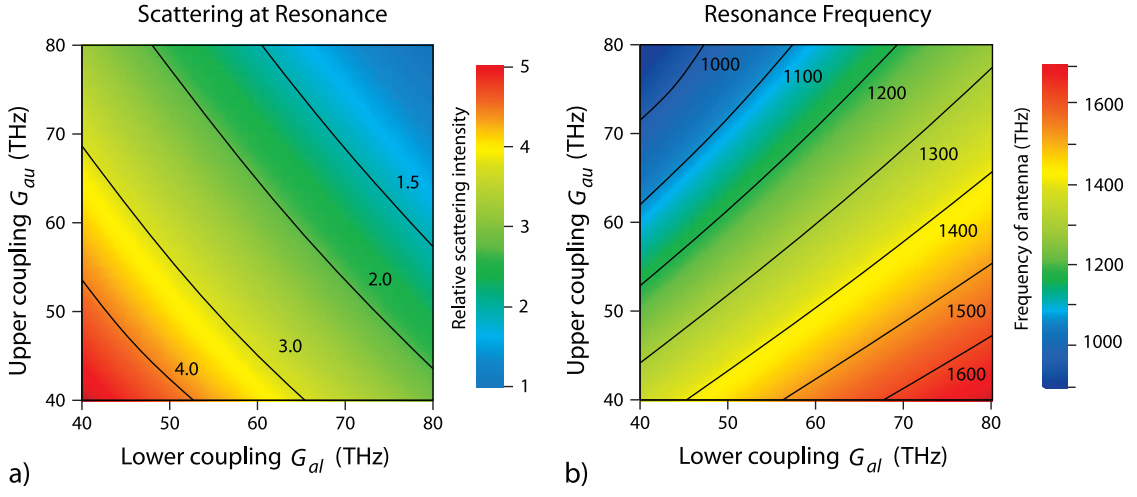

Figure 4. Dependence of (a) the scattering intensity at resonance and (b) resonance frequency ω_R of the central peak for a range of coupling coefficients G_{al} and G_{au}. The coefficients have values typical of the data shown in Figure 3. In these calculations, Γ = 100 THz, ω_a = 1150 THz, ω_{ql} = 1050 THz, and ω_{qu} = 1200 THz. The data were calculated by finding the peak and its frequency from $|\tilde{a}_a(\omega_R)|^2 = 1/|\Delta|^2$ using eq 3 for Δ.

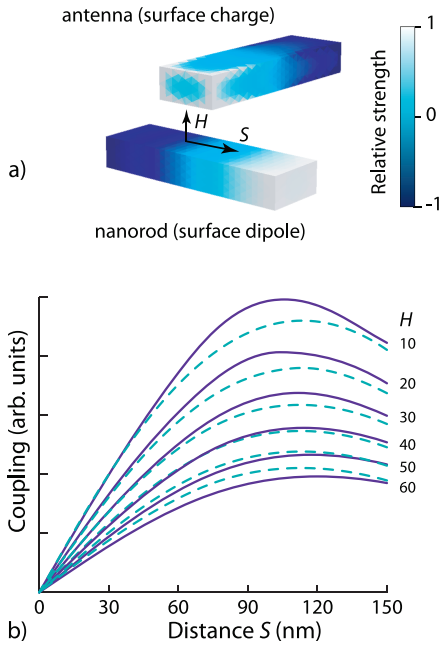

Figure 5. (a) Distribution of surface charges on the antenna and the surface dipoles on one of the quadrupole nanorods, calculated using an electrostatic eigenmode method. (b) Coulomb coupling between the antenna and one of the quadrupole nanorods as a function of distance $s = S$ for different heights H. The nanorods were 40 nm thick, 80 nm wide, and 260 nm long. The solid curves were calculated using the electrostatic eigenmode method and the dashed curves based on eq 7 using $h = H + H_0$ with $H_0 = 40$ nm and $L = 260$ nm.

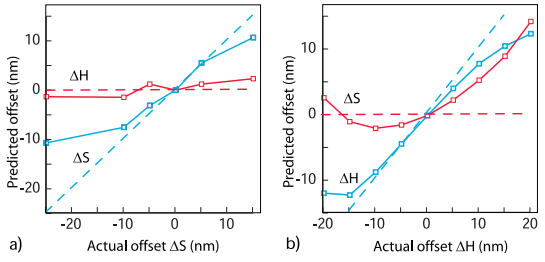

Figure 6. Predicted changes ΔS and ΔH in the position of the center antenna corresponding to (a) variations in S only (Figure 3a,b) and variations in H only (Figure 3b) (see text for details). The data points correspond to the table entries for each coupling coefficient with the solid lines as guides for the eye. Each dashed line represents the locus of the actual change in the position.

surface dipole distribution τ_q on particle q, as discussed in the Methods section. That is, the eigenfunctions represent the distributions of surface charge and surface dipoles associated with the localized surface plasmon modes. Examples of the surface eigenfunctions are shown in Figure 5a. For the fundamental resonance shown, the surface dipole distribution appears as a standing wave with an approximately sinusoidal dependence on position. Assuming that the dominant interaction of this surface dipole distribution is with the surface charge at one end of the upper nanorod, we propose the following approximate form for the coupling to a nanorod of length L:

$$G_{qa} \propto \frac{\sin(\pi s/L)}{h(s^2 + h^2 + L^2)} \tag{7}$$

This equation gives a reasonable fit to the position dependence of the coupling, shown in Figure 5b, as a function of $s = S$ for different heights H where $h = H + H_0$ is the center-to-center distance between the two nanorods. The equation is more accurate when h is small compared to L.

If we place the lower quadrupoles at position $(S_l,-H_0)$ in the $x-z$ plane and the upper quadrupoles at position (S_u,H_0) then for both s and h much smaller than L we would expect the coupling coefficients to vary as

$$G_{al} \approx G_{l0}\frac{\pi(S - S_l)}{L^3(H_0 + H)} \tag{8}$$

and

$$G_{au} \approx G_{u0}\frac{\pi(S - S_u)}{L^3(H_0 - H)} \tag{9}$$

where G_{l0} and G_{u0} are constants. Then the fractional changes $\Delta G_{al}/G_{al}$ and $\Delta G_{au}/G_{au}$ of the coupling with small changes ΔS and ΔH are

$$\frac{\Delta G_{al}}{G_{al}} \approx \frac{\Delta S}{S - S_l} - \frac{\Delta H}{H_0 + H} \tag{10}$$

and

$$\frac{\Delta G_{au}}{G_{au}} \approx \frac{\Delta S}{S - S_u} + \frac{\Delta H}{H_0 - H} \tag{11}$$

It is straightforward to invert eq 10 and eq 11 to write the changes in position ΔS and ΔH in terms of the relative changes in the coupling coefficients. If the position S and H of the center nanorod is known initially, then the motion of the nanorod about this position can be inferred from the changes ΔG_{al} and ΔG_{au} obtained from the spectra. As an example, we have used the coupling coefficients obtained from the parameter fits to the plasmon ruler spectra in Figure 3 (see Table 1 and Table 2) to estimate the change in position of the center nanorod. The estimates of the distance changes are obtained relative to the center nanorod initially at known positions (a) $S = 25$ nm and $H = 0$ with $S_l = 0$, $S_u = -35$, and $H_0 = 70$ nm for the data from Table 1, and (b) $S = 50$ nm and $H = 0$ with $S_l = 0$, $S_u = -35$, and $H_0 = 70$ nm for the data from Table 2. The fractional changes in the coupling coefficients are taken relative to G_{al} and G_{au} evaluated at these initial points and the changes in the position of the center nanorod are computed.

The results are compared with the known positions in Figure 6. The predictions of the changes ΔS and ΔH agree remarkably well with the actual changes over the regions where the model spectra fit well to the actual spectra. In particular, the predictions based on Figure 3b are reasonable in the region between

$H = -10$ nm and $H = 5$ nm corresponding to good fits of the analytical model to the spectra. Outside this region, the predictions are less accurate and our analytical model predicts a shift in the lateral displacement S when there should be none. This can be traced back to the reduced accuracy in the fit of the analytical model to the numerical data. Since the central resonance is the main feature that encodes both S and H, it is important that the analytical model reproduces the frequency and strength of this resonance. From Figure 3b, it is clear that the analytical model does not model the central resonance very well for large displacements—both the strength and frequency of the central resonance change with H. This is reflected in the results shown in Figure 6b. Note that the predictions in Figure 6 are based on first derivatives of the approximate expressions eq 8 and eq 9. In this regard, it is not surprising that the predictions are in error for large distance changes.

The important point is that we have been able to estimate the position of the center nanorod from the measured spectra. Key to achieving this is some knowledge of the initial location of the center dipole relative to the two quadrupole nanorod pairs. In this regard, the quadrupoles act as reference points for the ruler. Changes in the positions of the upper and lower quadrupoles relative to the antenna will affect the spectra since the couplings G_{au} and G_{al} will change. In this case, it would be impossible to distinguish between the motion of the antenna and the motion of the quadrupoles. These should remain fixed with respect to one another. How this is achieved in practice depends on the means by which the plasmonic ruler has been fabricated. Moreover, we have assumed that the Coulomb coupling between the upper and lower quadrupoles is small. If we take this coupling into account in deriving eq 3, we find that the excitation of the central dipole antenna depends on differences $G_{13} - G_{14}$ between the direct coupling G_{13} and the cross-coupling G_{14} and likewise for $G_{24} - G_{23}$. This partial cancellation makes the ruler less sensitive to the interactions between the upper and lower quadrupoles.

CONCLUSIONS

In conclusion, we have shown that it is possible to model a 3D plasmonic oligomer that is used as a 3D plasmonic ruler by an electrostatic approximation. In particular, we derived analytical expressions that represent scattering intensity, resonance frequencies, and coupling strength of spectral features of the high-resolution plasmon-induced transparency spectra. Our method proves that for small deviations there exists a unique relationship to encode in the scattering spectra the lateral displacement S and vertical displacement H of the 3D plasmonic ruler. Using an approximation to the position dependence of the electrostatic coupling between the nanorods, we have shown that it is possible to estimate the position of the central nanorod using the measured spectra. Our work has dramatic consequences for the simplified and time-efficient use of 3D plasmonic rulers as sensitive tools to measure structural changes and their dynamics in complex macromolecules, DNA scaffolds, proteins, and other biological systems.

METHODS

The mathematical analysis of the three-dimensional plasmonic ruler is based on an electrostatic method[14,15] that describes the Coulomb interaction between the localized surface plasmons. The method gives the excitation amplitude of the antenna when coupled to the other nanorods, which has the form $\tilde{a}_a = A_a/\Delta$, where Δ is given by eq 3. The transmission spectrum has the form $I_{max} - A_a^2/|\Delta|^2$, which is fitted to the experimental and numerical data of Liu *et al.*[5] The fitted parameters are given in Table 1 and Table 2.

The dependence of the coupling on the position of the central nanorod is given in the electrostatic formalism in terms of the electric field from a surface charge distribution σ_a on particle a interacting with the surface dipole distribution τ_q on particle q. The coupling G_{qa} between the antenna a and one of the other nanorods q takes the form

$$G_{qa} \propto \oint\oint \frac{\tau_q(\vec{r}_q)\hat{n}_q.(\vec{r}_q - \vec{r}_a)\sigma_a(\vec{r}_a)}{|\vec{r}_q - \vec{r}_a|^3} dS_a dS_q \qquad (12)$$

where $\hat{n}_q$ is surface normal at $\vec{r}_q$ on particle q. This expression is usually evaluated numerically—an example is shown in Figure 5b. A clue to the dependence of the coupling on the position of the central nanorod is obtained by assuming that the surface charge on the antenna is located predominantly at the ends. Then the integral over the antenna surface can be approximated by a charge located at $\vec{r}_a = s\hat{x} + h\hat{z}$. The surface dipole distribution for the fundamental resonant mode appears like a standing wave with an approximate form $\tau_q(x) = \tau_0 \sin(\pi x/L)$, where L is the length of the nanorod (Figure 5a). This is zero at the center of the nanorod and maximum at the ends. Using the normal of the nanorod surface closest to the antenna $\hat{n}_q = \hat{z}$, the coupling is given approximately by

$$G_{qa} \propto -h \int_{-L/2}^{L/2} \frac{\sin(\pi x/L)}{((x-s)^2+h^2)^{3/2}} dx \qquad (13)$$

Despite the approximations which have been used to derive eq 13, there is no simple solution. However, the form of the integral suggests the approximate form given in eq 7. As discussed above, this equation gives a reasonable fit to the position dependence of the coupling, shown in Figure 5b, as a function of $s = S$ for different heights H where $h = H + H_0$ is the center-to-center distance between the two nanorods. The equation is more accurate when h is small compared to L.

Acknowledgment. We acknowledge funding through DFG (FOR 730/SPP1391/Gi269-M/1), BMBF (3D Metamaterial), and the MPI FKF-University guest professorship program.

REFERENCES AND NOTES

1. Sönnichsen, C.; Reinhard, B. M.; Liphardt, J.; Alivisatos, A. P. A Molecular Ruler Based On Plasmon Coupling of Single

Gold and Silver Nanoparticles. *Nat. Biotechnol.* **2005**, *23*, 741–745.
2. Reinhard, B. M.; Siu, M.; Agarwal, H.; Alivisatos, A. P.; Liphardt, J. Calibration of Dynamic Molecular Rulers Based on Plasmon Coupling between Gold Nanoparticles. *Nano Lett.* **2005**, *5*, 2246–2252.
3. Jain, P. K.; Huang, W.; El-Sayed, M. A. On the Universal Scaling Behavior of the Distance Decay of Plasmon Coupling in Metal Nanoparticle Pairs: A Plasmon Ruler Equation. *Nano Lett.* **2007**, *7*, 2080–2088.
4. Tabor, C.; Murali, R.; Mahmoud, M.; El-Sayed, M. A. On the Use of Plasmonic Nanoparticle Pairs As a Plasmon Ruler: The Dependence of the Near-Field Dipole Plasmon Coupling on Nanoparticle Size and Shape. *J. Phys. Chem. A* **2009**, *113*, 1946–1953.
5. Liu, N.; Alivisatos, A. P.; Hentschel, M.; Weiss, T.; Giessen, H. Three-Dimensional Plasmon Rulers. *Science* **2011**, *332*, 1407–1410.
6. Liu, N.; Langguth, L.; Weiss, T.; Kästel, J.; Fleischhauer, M.; Pfau, T.; Giessen, H. Plasmonic Analogue of Electromagnetically Induced Transparency at the Drude Damping Limit. *Nat. Mater.* **2009**, *8*, 758–762.
7. Papasimakis, N.; Fedotov, V. A.; Zheludev, N. I.; Prosvirnin, S. L. Metamaterial Analog of Electromagnetically Induced Transparency. *Phys. Rev. Lett.* **2008**, *101*, 253903.
8. Zhang, S.; Genov, D. A.; Wang, Y.; Liu, M.; Zhang, X. Plasmon-Induced Transparency in Metamaterials. *Phys. Rev. Lett.* **2008**, *101*, 047401.
9. Tassin, P.; Zhang, L.; Koschny, T.; Economou, E. N.; Soukoulis, C. M. Low-Loss Metamaterials Based on Classical Electromagnetically Induced Transparency. *Phys. Rev. Lett.* **2009**, *102*, 053901.
10. Liu, N.; Weiss, T.; Mesch, M.; Langguth, L.; Eigenthaler, U.; Hirscher, M.; Sönnichsen, C.; Giessen, H. Planar Metamaterial Analogue of Electromagnetically Induced Transparency for Plasmonic Sensing. *Nano Lett.* **2010**, *10*, 1103–1107.
11. Luk'yanchuck, B.; Zheludev, N. I.; Maier, S. A.; Halas, N. J.; Nordlander, P.; Giessen, H.; Chong, C. T. The Fano Resonance in Plasmonic Nanostructures and Metamaterials. *Nat. Mater.* **2010**, *9*, 707–715.
12. Artar, A.; Yanik, A. A.; Altug, H. Multispectral Plasmon Induced Transparency in Coupled Meta-Atoms. *Nano Lett.* **2011**, *11*, 1685–1689.
13. Wu, C.; Khanikaev, A. B.; Shvets, G. Broadband Slow Light Metamaterial Based on a Double-Continuum Fano Resonance. *Phys. Rev. Lett.* **2011**, *106*, 107403.
14. Davis, T. J.; Vernon, K. C.; Gómez, D. E. Designing Plasmonic Systems Using Optical Coupling between Nanoparticles. *Phys. Rev. B* **2009**, *79*, 155423.
15. Davis, T. J.; Gómez, D. E.; Vernon, K. C. Simple Model for the Hybridization of Surface Plasmon Resonances in Metallic Nanoparticles. *Nano Lett.* **2010**, *10*, 2618–2625.